Supporting information

Hg^{2+} and Cd^{2+} binding of a bioinspired hexapeptide with two cysteine units constructed as a minimalistic metal ion sensing fluorescent probe

Levente I. Szekeres, Sára Bálint, Gábor Galbács, Ildikó Kálomista, Tamás Kiss, Flemming H. Larsen, Lars Hemmingsen, Attila Jancsó*

- Table S1. pK_a values for the deprotonation processes leading to the various mono and bis complexes formed in the Hg^{2+}:DY system (with their errors in parentheses, last digit) (I = 0.1 M $NaClO_4$, T = 298 K).
- Table S2. Overall formation constants (logβ) of the species formed in the Hg^{2+}:DY system calculated by using different, fixed "arbitrary" logβ values for the HgH_2L complex and pK_a values characterizing the deprotonation processes of the various mono and bis complexes.
- Figure S1. UV absorption spectra of DY as a function of pH, in the range of pH = 1.87 to 10.89 (c_{DY} = 1×10^{-4} M, T = 298 K).
- Figure S2. UV absorption spectra recorded in the Hg^{2+}:DY 0.5:1 (A) and 1:1 (B) systems as a function of pH, in the ranges of pH = 1.83 to 10.87 (A) and pH = 1.83 to 10.95 (B) (c_{DY} = 1×10^{-4} M, T = 298 K). Dashed and dotted lines show the spectra of the free DY at pH = 1.87 and Hg^{2+}:DY 0.5:1 at pH = 1.83, respectively.
- Difference UV absorption spectra for the Hg^{2+}:DY 1:1 (pH = 6.0, continuous line) and 0.5:1 (pH = 9.5, dashed line) systems calculated by subtracting the spectra of the free ligand recorded at the same pH and concentration as those of the relevant Hg^{2+}:DY samples. The calculated difference spectra are normalized for the metal ion concentration.
- Figure S4. UV absorption spectra recorded in the Cd^{2+}:DY 0.5:1 (A) and 1:1 (B) systems as a function of pH, in the ranges of pH = 2.00 to 11.07 (A) and pH = 2.01 to 10.97 (B) (c_{DY} = 5×10^{-5} M, T = 298 K).
- Figure S5. Assignment of the various ^{1}H NMR resonances of DY at pH = 5.7 (H_2O:D_2O = 90:10 % v/v, c_{DY} = 1.0×10^{-3} M, T = 298 K).
- Figure S6. Part of the ^{1}H NMR spectra of DY, recorded as a function of pH, displaying resonances of the $C_\beta H_2$ hydrogen atoms of the Asp, Cys and Tyr residues (A) and those of the amide groups and the aromatic ring of Tyr (B) (H_2O:D_2O = 90:10 % v/v, c_{DY} = 1.0×10^{-3} M, T = 298 K).
- Figure S7. Part of the ^{1}H NMR spectra, recorded in the Hg^{2+}:DY 0.5:1 system as a function of pH, displaying resonances of the $C_\beta H_2$ hydrogen atoms of the Asp, Cys and Tyr residues

(A) and those of the amide groups and the aromatic ring of Tyr (B) (H_2O:D_2O = 90:10 % v/v, c_{DY} = 1.0×10^{-3} M, T = 298 K).

- Figure S8. Part of the ^{1}H NMR spectra, recorded in the Hg^{2+}:DY 1:1 system as a function of pH, displaying resonances of the $C_\beta H_2$ hydrogen atoms of the Asp, Cys and Tyr residues (A) and those of the amide groups and the aromatic ring of Tyr (B) (H_2O:D_2O = 90:10 % v/v, c_{DY} = 1.0×10^{-3} M, T = 298 K).
- Figure S9. Part of the ^{1}H NMR spectra recorded at pH = 7.0 in the Cd^{2+}:DY system as a function of the Cd^{2+}:DY ratio (H_2O:D_2O = 90:10 % v/v, c_{DY} = 1.0×10^{-3} M, T = 298 K).
- Figure S10. Fluorescence titration of DY by Cd^{2+} at pH = 7.1 (c_{DY} = 3.0×10^{-5} M, λ_{EM} = 308 nm, λ_{EX} = 278 nm). The inset represent the change of the recorded spectra as a function of increasing Cd^{2+}:DY ratio.
- Figure S11. Hg^{2+} binding to the immobilized ligand (μmol) as a function of pH (V_{sample} = 10.0 mL, containing n = 2.27 μmol Hg^{2+}; $m_{DY\text{-}NTG}$ = 10.0 mg; $c_{Ac/NaOAc}$ = 0.02 M (pH = 4.0), c_{MES} = 0.02 M (pH = 6.0).
- Scheme S1. Proposed schematic structures for the Hg^{2+}:DY complexes.
- Scheme S2. Proposed schematic structures for the Cd^{2+}:DY complexes.

Table S1: pK_a values for the deprotonation processes leading to the various mono and bis complexes formed in the Hg^{2+}:DY system (with their errors in parentheses, last digit) (I = 0.1 M $NaClO_4$, T = 298 K, number of data points used in the fitting = 164, fitting parameter = 0.005 cm^3). The logβ of the HgH_2L complex (logβ_{HgH_2L}) was estimated from the stability constant determined by Iranzo et al.[1] for the parent mono complex (HgL) of the terminally protected CDPPC peptide (log$K$ = 40.0). We assumed the same stability constant for the Hg^{2+} + $[H_2L]^{2-}$ = $[HgH_2L]$ process of DY, allowing to set a value for logβ_{HgH2L} according to the equation given in the footnote of the Table. Please also note that data evaluation required the fixing of this estimated formation constant.

Species	p$K_a^{HgH_yL_z}$ [a]
HgH_2L	4.1(1)
$[HgHL]^-$	9.6(1)
$[HgL]^{2-}$	–
$[HgH_3L_2]^{3-}$	7.9(3)
$[HgH_2L_2]^{4-}$	10.0(2)
$[HgHL_2]^{5-}$	11.2(3)
$[HgL_2]^{6-}$	–
logβ_{HgH_2L}	53.85 [b]

[a] Data refer to the following deprotonation processes: $HgH_yL_z = HgH_{y-1}L_z + H^+$; [b] For estimating the logβ value of HgH_2L the following equation was used: log$K_{Hg(CDPPC)}$ = logK_{HgH_2L} = logβ_{HgH_2L} – log$\beta_{[H_2L]^{2-}}$ where L stands for the fully deprotonated DY ligand.

1, S. Pires, J. Habjanič, M. Sezer, C. M. Soares, L. Hemmingsen and O. Iranzo, *Inorg. Chem.*, 2012, **51**, 11339–11348.

Table S2: Overall formation constants (logβ) of the species formed in the Hg^{2+}:DY system calculated by using different, fixed "arbitrary" logβ values for the HgH_2L complex and pK_a values characterizing the deprotonation processes of the various mono and bis complexes. The first model is the same as presented in Table S1. The $\log\beta_{HgH_2L}$ value, used in the first model, was decreased and increased by 5 log units in the calculations of models 2 and 3, respectively. $\log\beta_{HgH_2L}$ in model 4 was set to a value that resulted in free Hg^{2+} ions appearing in a notable amount (ca. 0.16 mole fraction $[Hg^{2+}]_{freel}$) at pH = 2.0 and 1:1 Hg^{2+}:DY ratio.

	1		2		3		4	
Species	logβ	pK_a^{HgHyLz} [a]	logβ	pK_a^{HgHyLz} [a]	logβ	pK_a^{HgHyLz} [a]	logβ	pK_a^{HgHyLz} [a]
HgH_2L	53.85 [b]	4.1	48.85 [b]	4.1	58.85 [b]	4.1	31.85 [b]	4.1
$[HgHL]^-$	49.7(1)	9.6	44.7(1)	9.6	54.7(1)	9.6	27.8(1)	9.6
$[HgL]^{2-}$	40.1(1)	–	35.1(1)	–	45.1(1)	–	18.2(1)	–
$[HgH_3L_2]^{3-}$	72.7(3)	7.9	67.7(3)	7.9	77.7(3)	7.9	50.7(2)	7.8
$[HgH_2L_2]^{4-}$	64.8(2)	10.0	59.8(2)	10.0	69.8(2)	10.0	42.9(1)	10.0
$[HgHL_2]^{5-}$	54.8(1)	11.2	49.8(1)	11.2	59.8(1)	11.2	32.9(1)	11.2
$[HgL_2]^{6-}$	43.6(3)	–	38.6(3)	–	48.6(3)	–	21.7(2)	–

[a] Data refer to the following deprotonation processes: $HgH_yL_z = HgH_{y-1}L_z + H^+$; [b] For estimating the logβ value of HgH_2L the following equation was used: $\log K_{Hg(CDPPC)} = \log K_{HgH_2L} = \log\beta_{HgH_2L} - \log\beta_{[H_2L]^{2-}}$ where L stands for the fully deprotonated DY ligand – see the reference for $\log K_{Hg(CDPPC)}$ under Table S1.

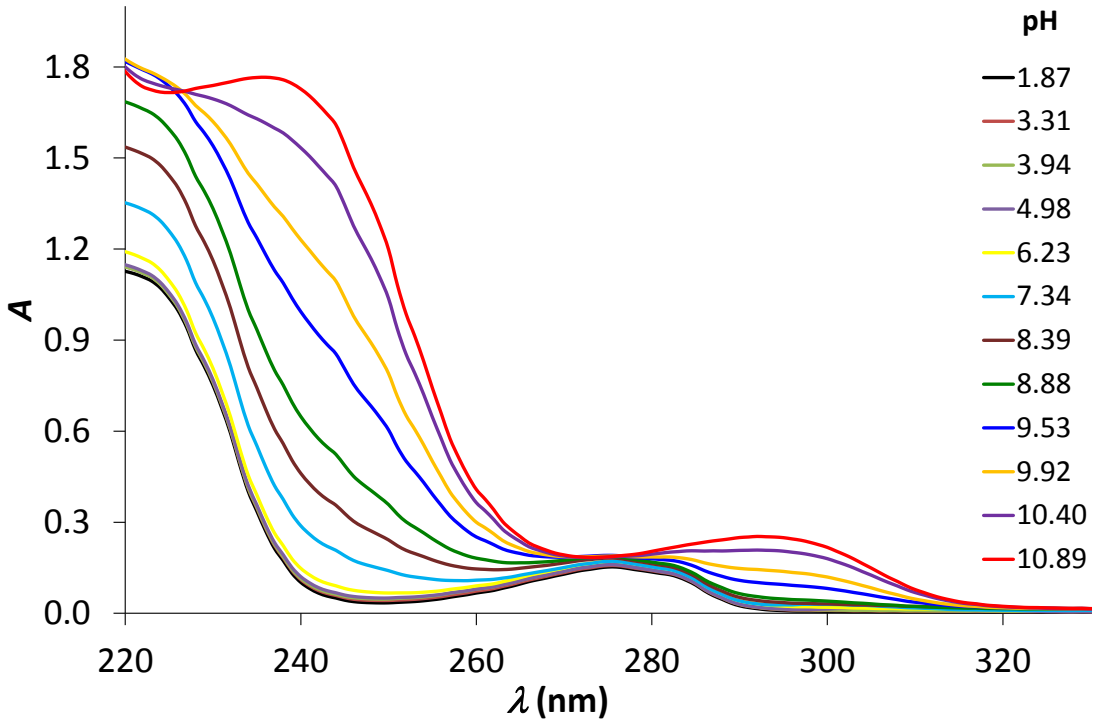

Figure S1. UV absorption spectra of DY as a function of pH, in the range of pH = 1.87 to 10.89 (c_{DY} = 1×10^{-4} M, T = 298 K).

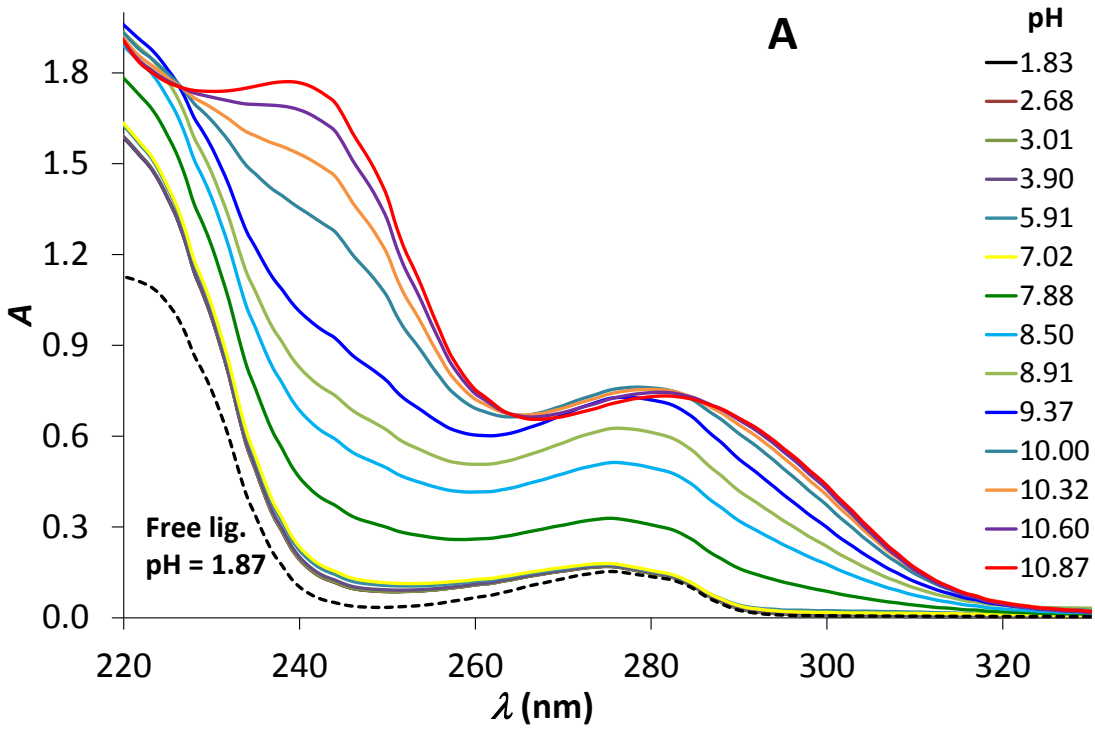

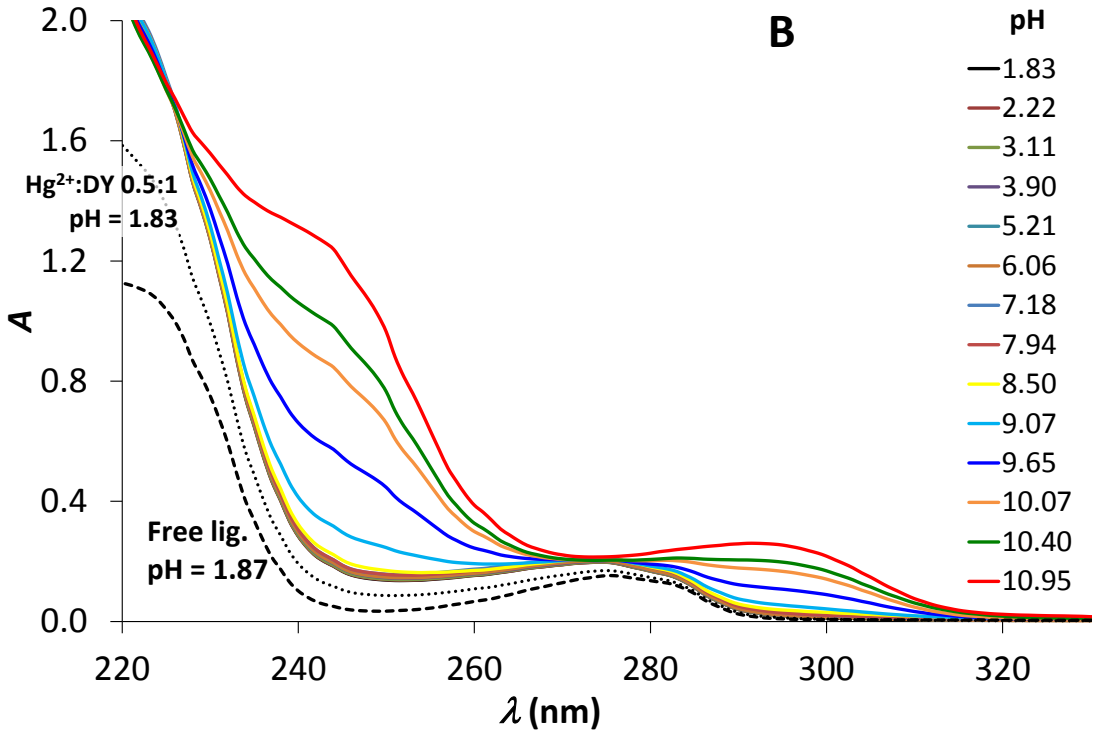

Figure S2. UV absorption spectra recorded in the Hg^{2+}:DY 0.5:1 (A) and 1:1 (B) systems as a function of pH, in the ranges of pH = 1.83 to 10.87 (A) and pH = 1.83 to 10.95 (B) (c_{DY} = 1×10^{-4} M, T = 298 K). Dashed and dotted lines show the spectra of the free DY at pH = 1.87 and Hg^{2+}:DY 0.5:1 at pH = 1.83, respectively.

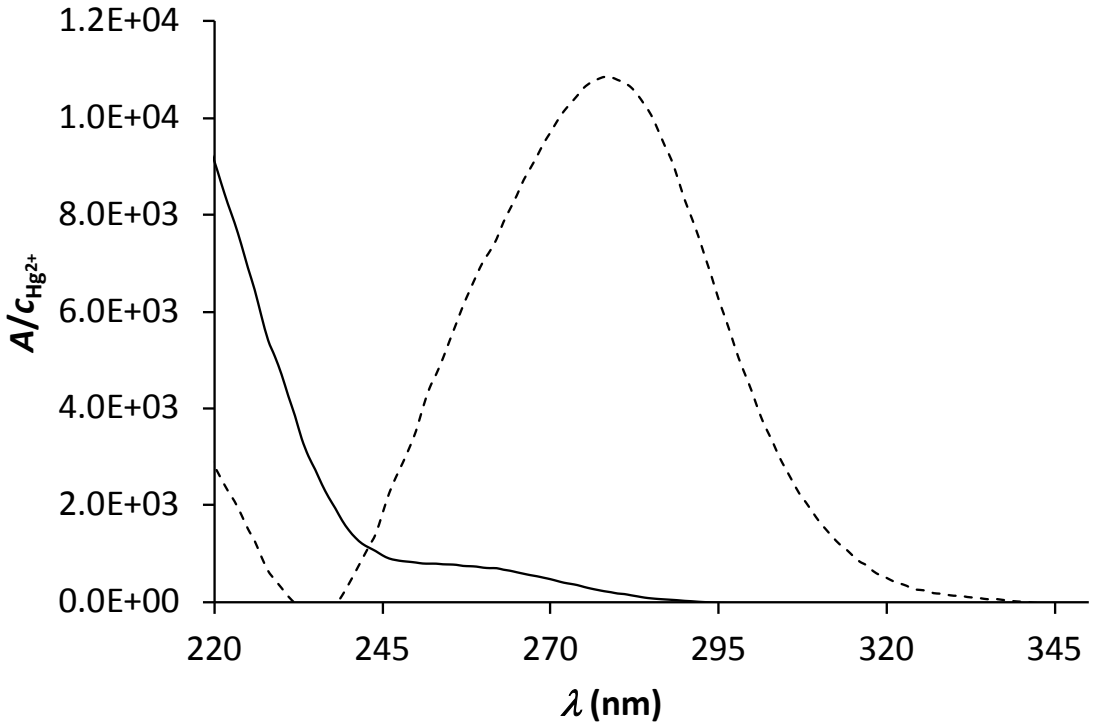

Figure S3. Difference UV absorption spectra for the Hg^{2+}:DY 1:1 (pH = 6.0, continuous line) and 0.5:1 (pH = 9.5, dashed line) systems calculated by subtracting the spectra of the free ligand recorded at the same pH and concentration as those of the relevant Hg^{2+}:DY samples. The calculated difference spectra are normalized for the metal ion concentration.

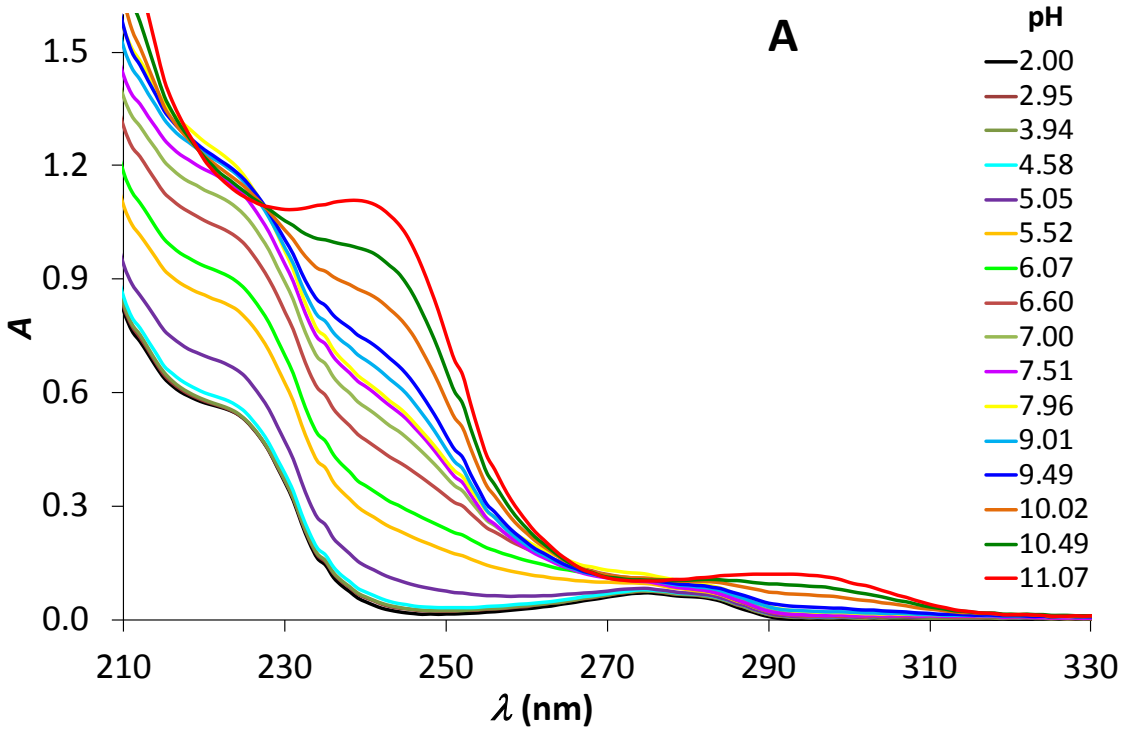

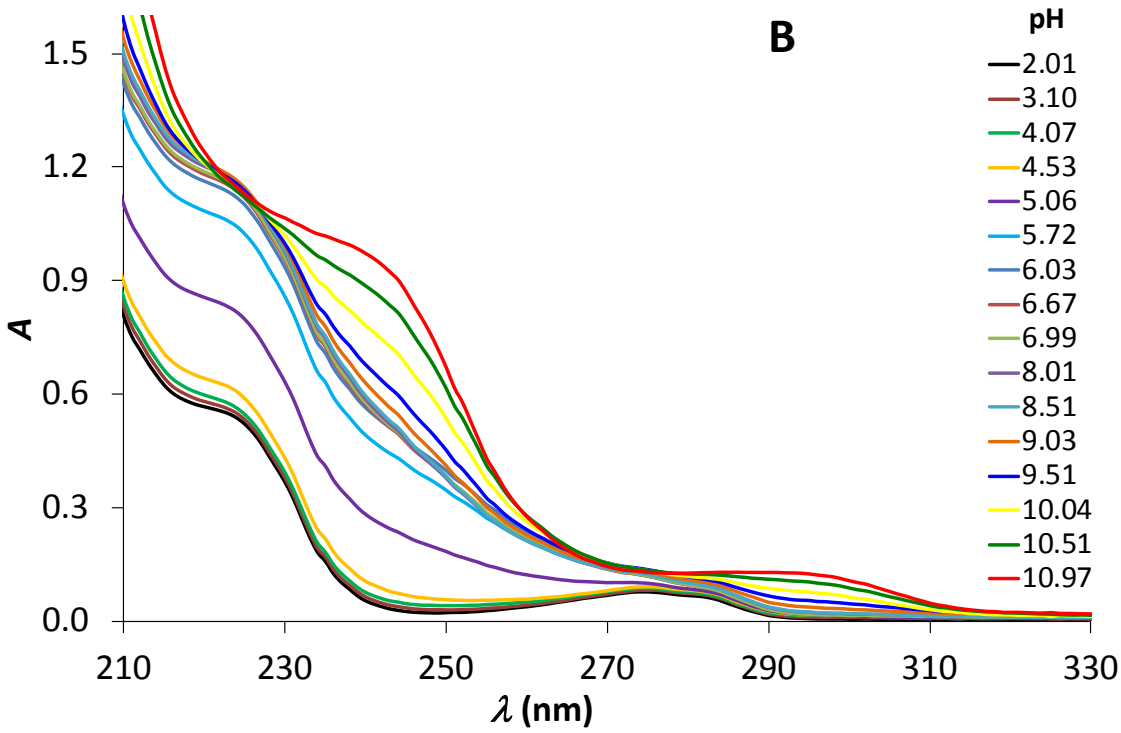

Figure S4. UV absorption spectra recorded in the Cd^{2+}:DY 0.5:1 (A) and 1:1 (B) systems as a function of pH, in the ranges of pH = 2.00 to 11.07 (A) and pH = 2.01 to 10.97 (B) (c_{DY} = 5×10^{-5} M, T = 298 K).

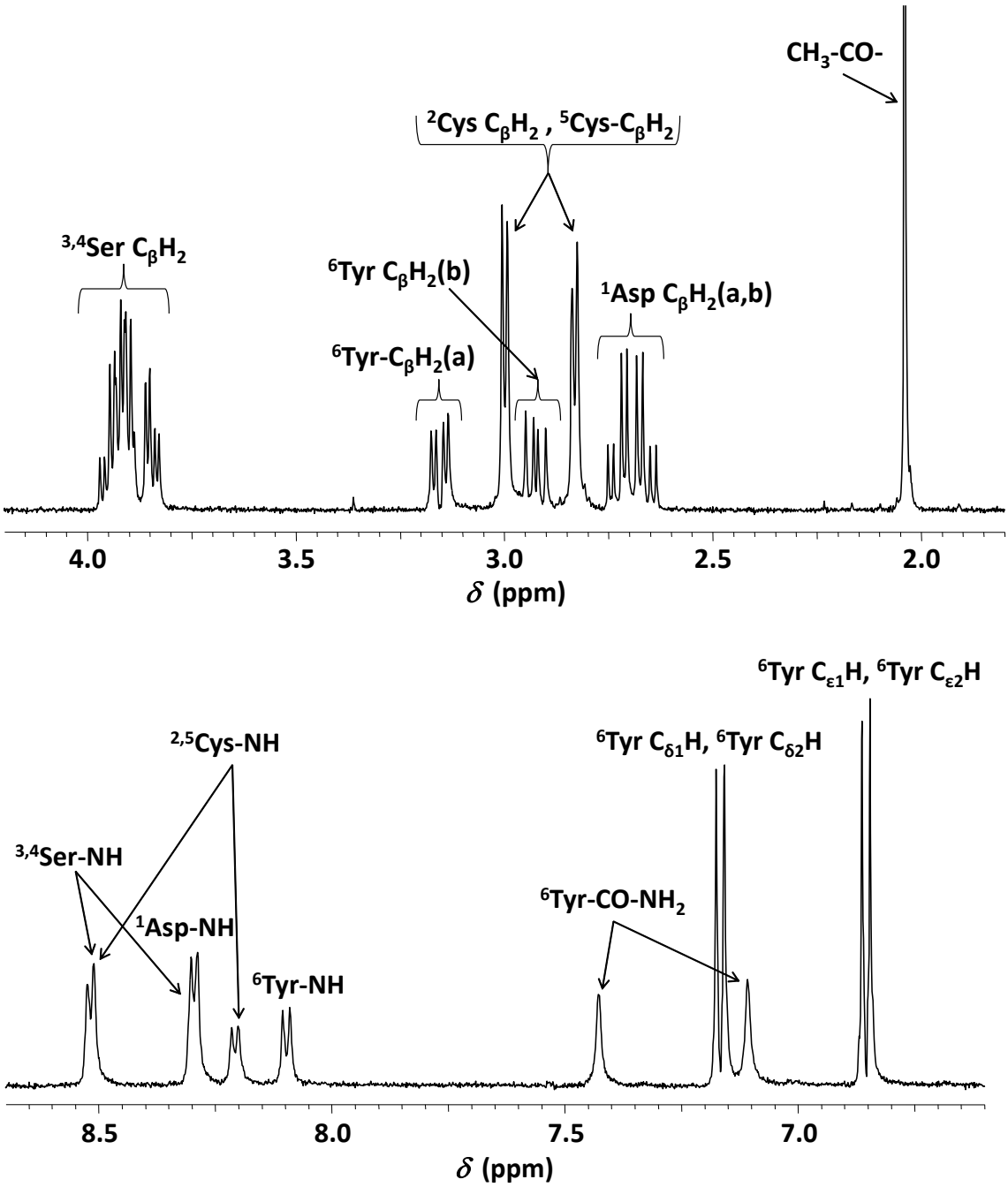

Figure S5. Assignment of the various ^{1}H NMR resonances of DY at pH = 5.7 (H_2O:D_2O = 90:10 % v/v, c_{DY} = 1.0×10^{-3} M, T = 298 K).

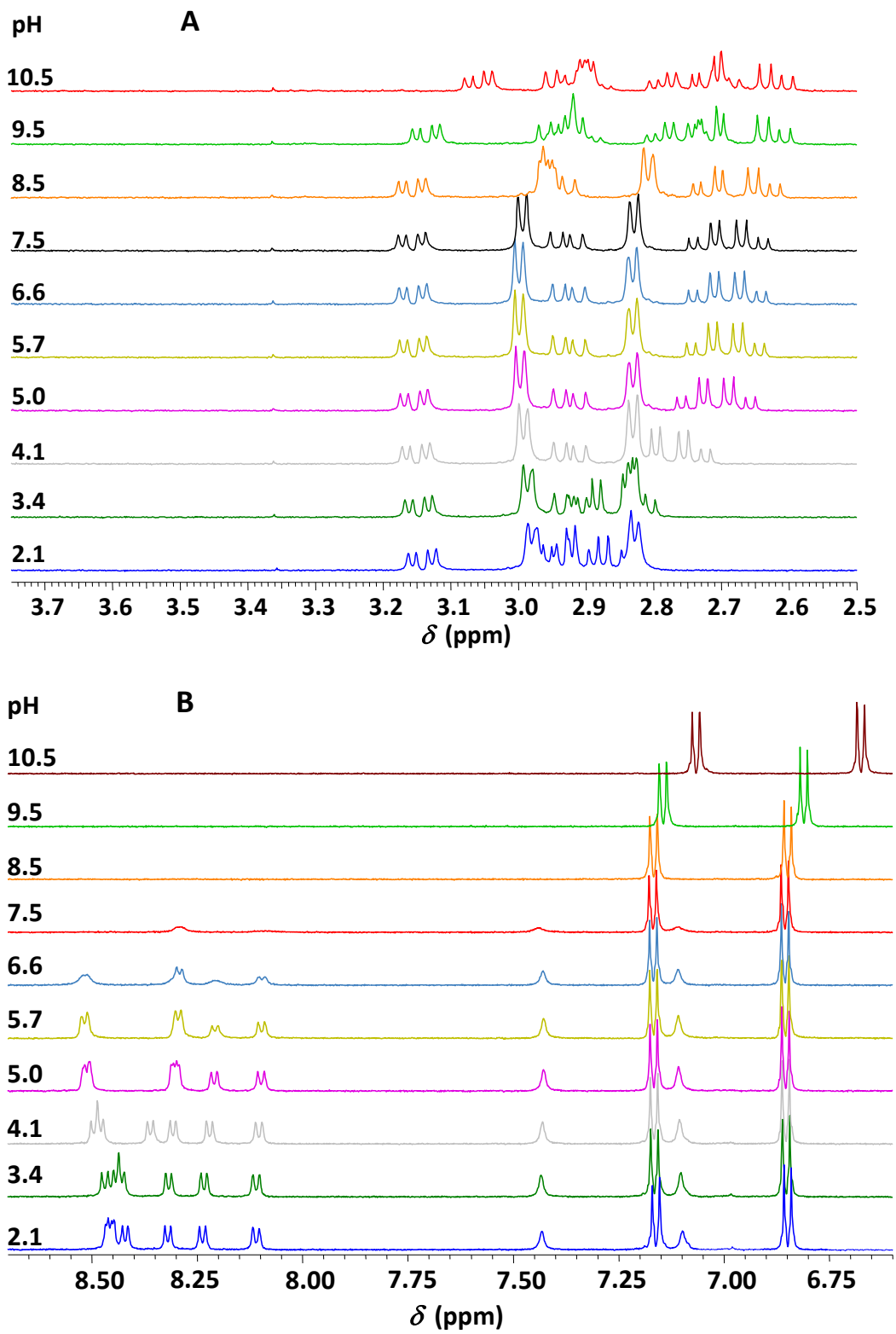

Figure S6. Part of the ^{1}H NMR spectra of DY, recorded as a function of pH, displaying resonances of the $C_{\beta}H_2$ hydrogen atoms of the Asp, Cys and Tyr residues (A) and those of the amide groups and the aromatic ring of Tyr (B) (H_2O:D_2O = 90:10 % v/v, c_{DY} = 1.0×10^{-3} M, T = 298 K).

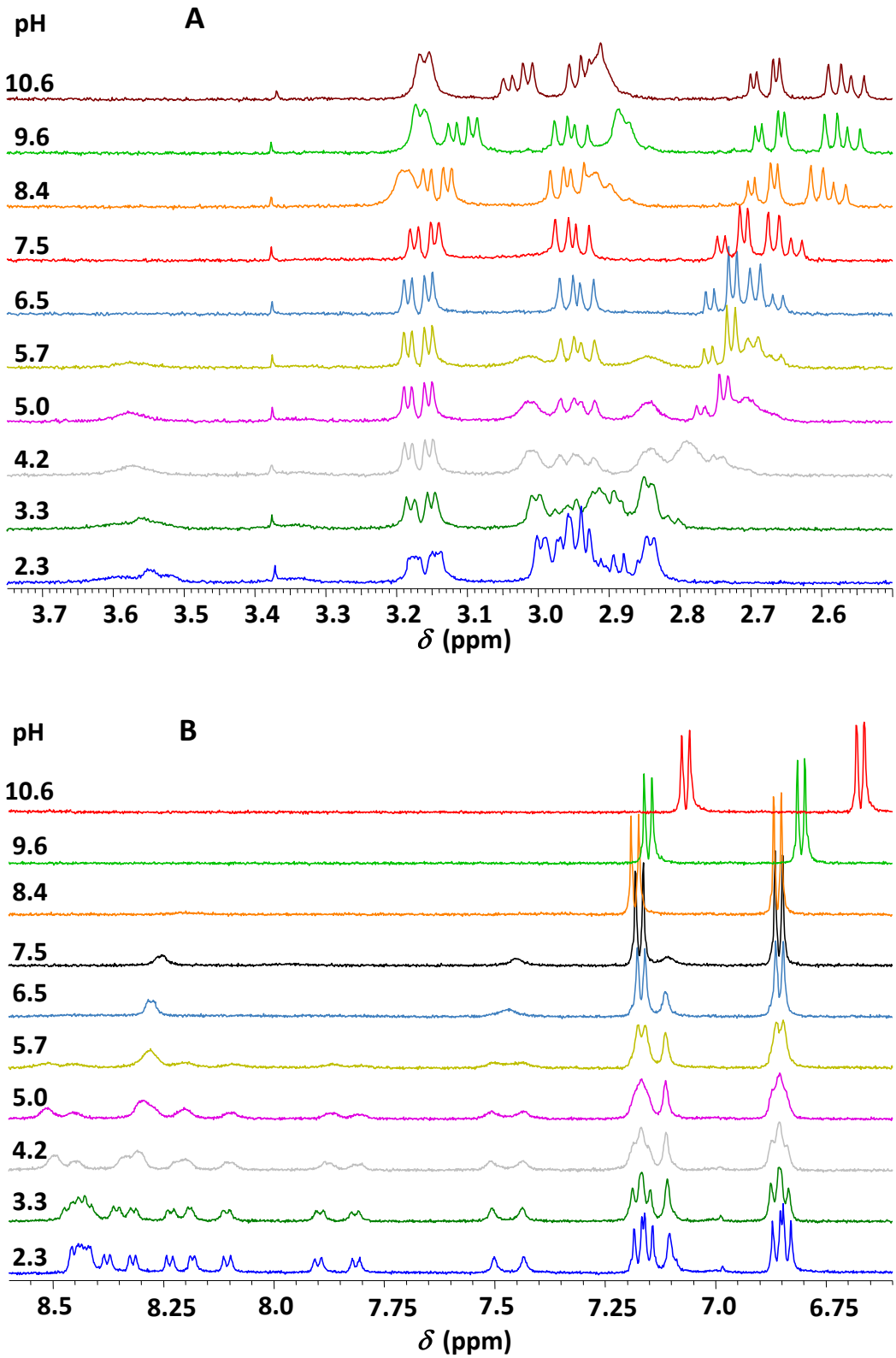

Figure S7. Part of the ^{1}H NMR spectra, recorded in the Hg^{2+}:DY 0.5:1 system as a function of pH, displaying resonances of the $C_{\beta}H_2$ hydrogen atoms of the Asp, Cys and Tyr residues (A) and those of the amide groups and the aromatic ring of Tyr (B) (H_2O:D_2O = 90:10 % v/v, c_{DY} = 1.0×10^{-3} M, T = 298 K).

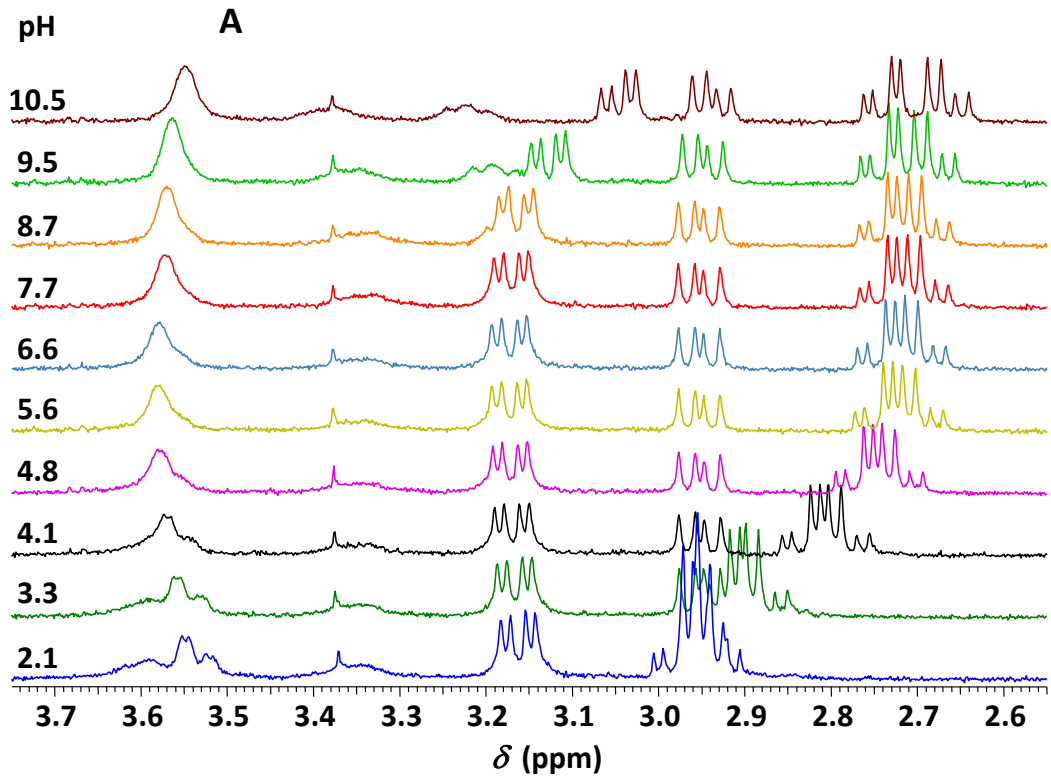

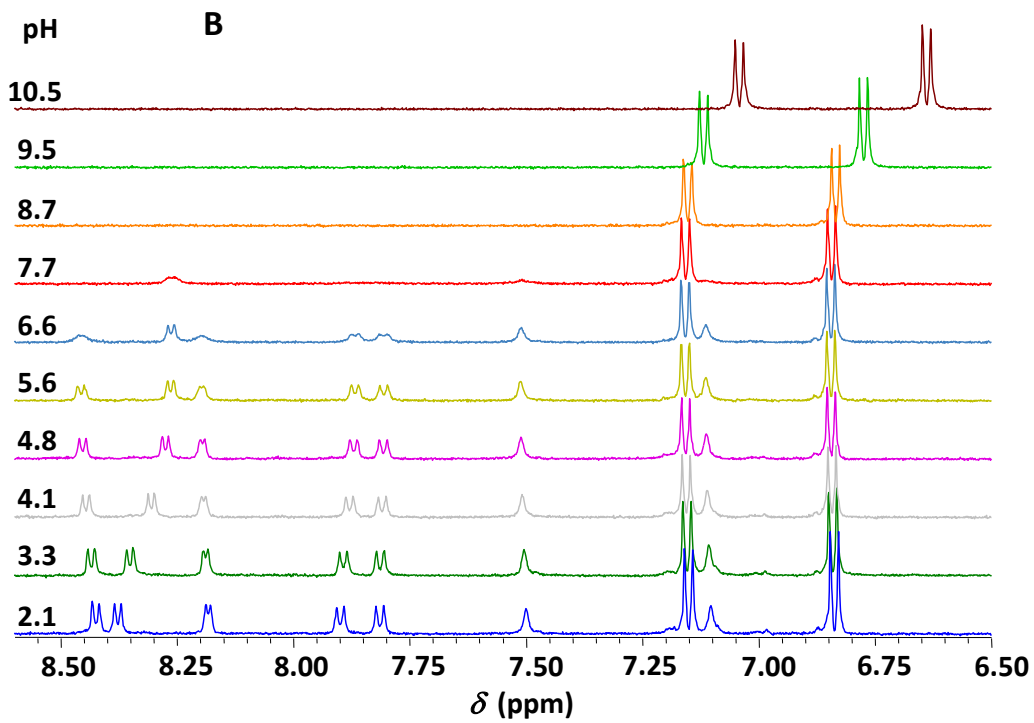

Figure S8. Part of the ^{1}H NMR spectra, recorded in the Hg^{2+}:DY 1:1 system as a function of pH, displaying resonances of the $C_{\beta}H_2$ hydrogen atoms of the Asp, Cys and Tyr residues (A) and those of the amide groups and the aromatic ring of Tyr (B) (H_2O:D_2O = 90:10 % v/v, c_{DY} = 1.0×10^{-3} M, T = 298 K).

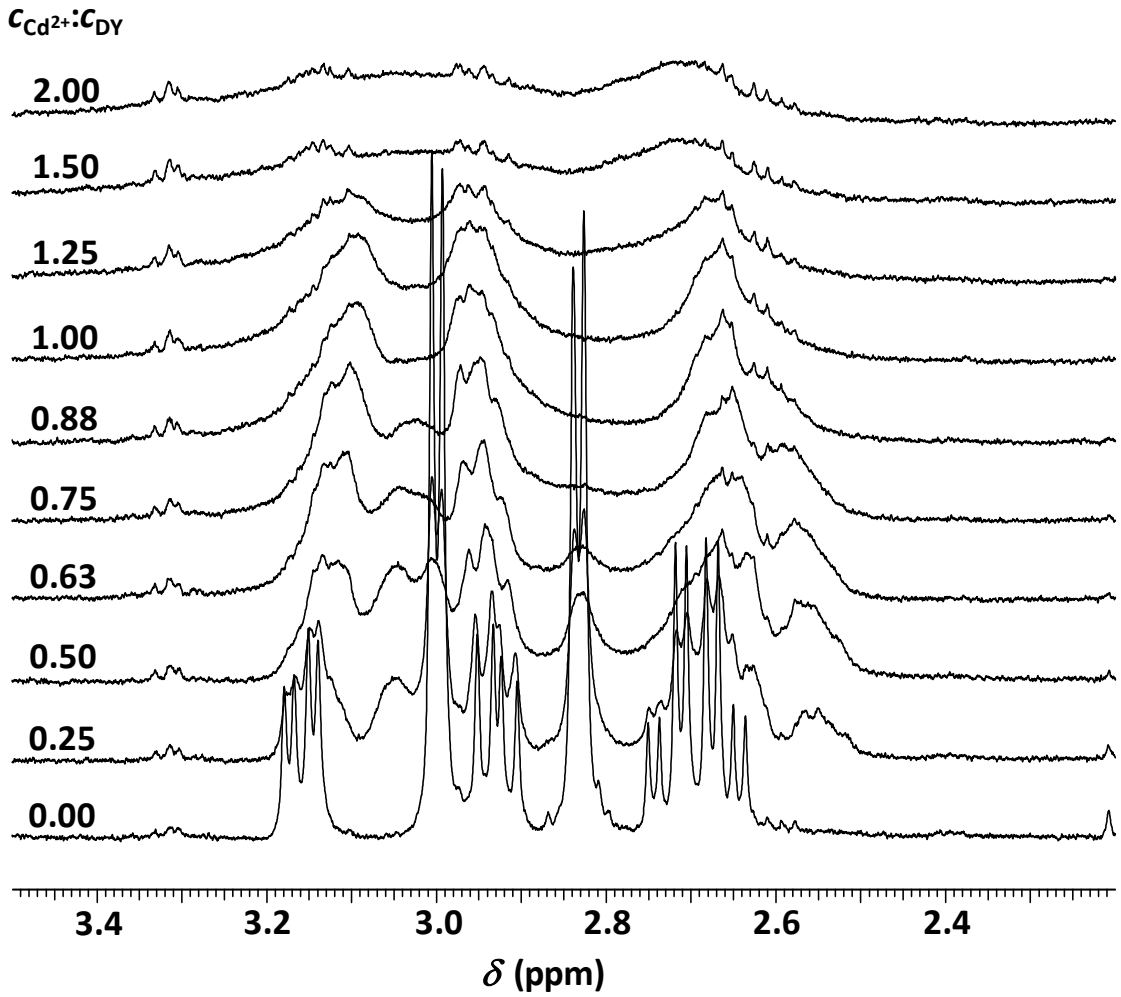

Figure S9. Part of the ^{1}H NMR spectra recorded at pH = 7.0 in the Cd^{2+}:DY system as a function of the Cd^{2+}:DY ratio (H_2O:D_2O = 90:10 % v/v, c_{DY} = 1.0×10^{-3} M, T = 298 K).

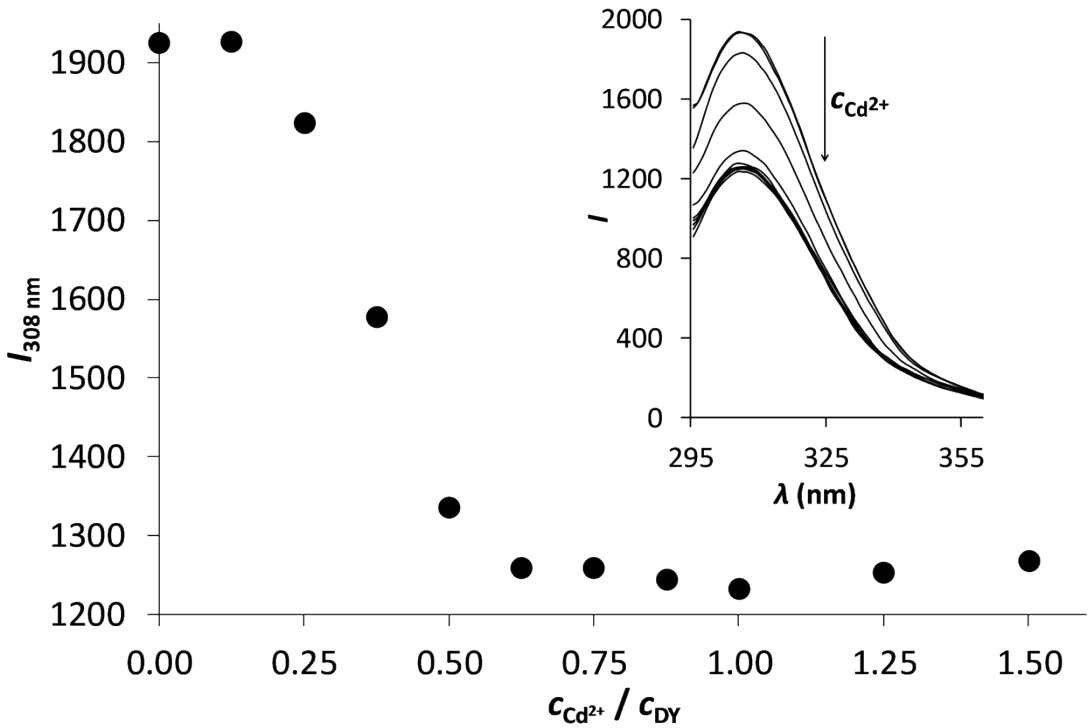

Figure S10. Fluorescence titration of DY by Cd^{2+} at pH = 7.1 (c_{DY} = 3.0×10^{-5} M, λ_{EM} = 308 nm, λ_{EX} = 278 nm). The inset shows the change of the recorded spectra as a function of increasing Cd^{2+}:DY ratio.

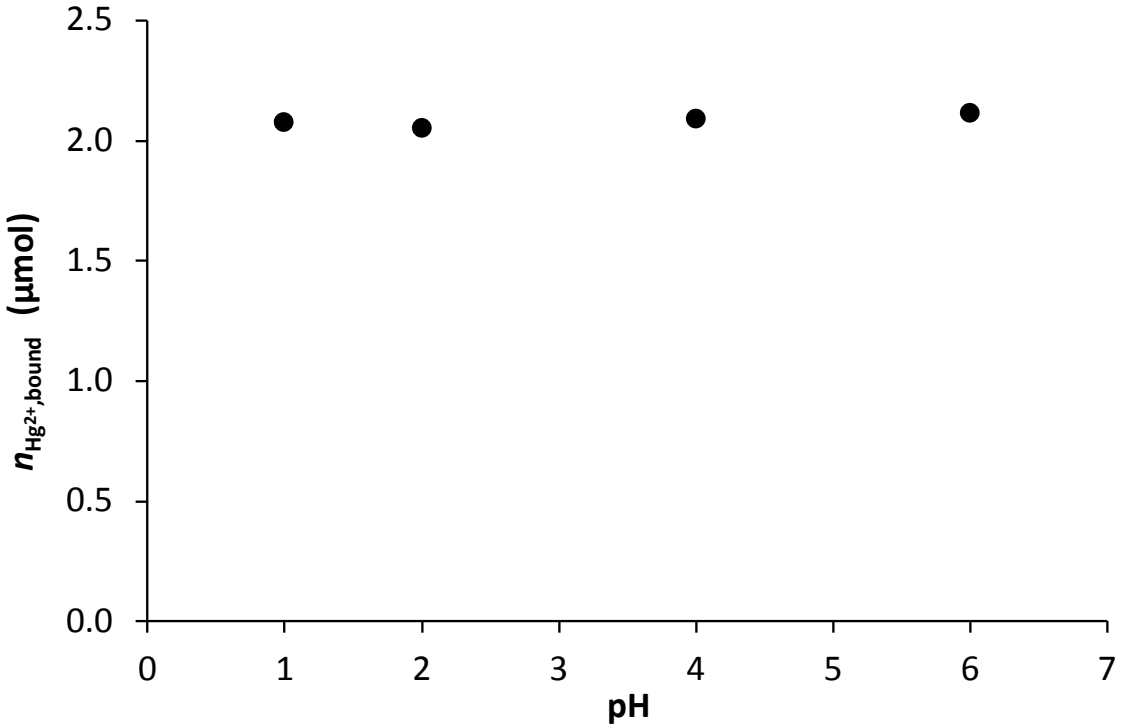

Figure S11. Hg^{2+} binding to the immobilized ligand (μmol) as a function of pH (V_{sample} = 10.0 mL, containing n = 2.2 μmol Hg^{2+}; $m_{DY\text{-}NTG}$ = 10.0 mg; $c_{AcOH/NaOAc}$ = 0.02 M (pH = 4.0), c_{MES} = 0.02 M (pH = 6.0).

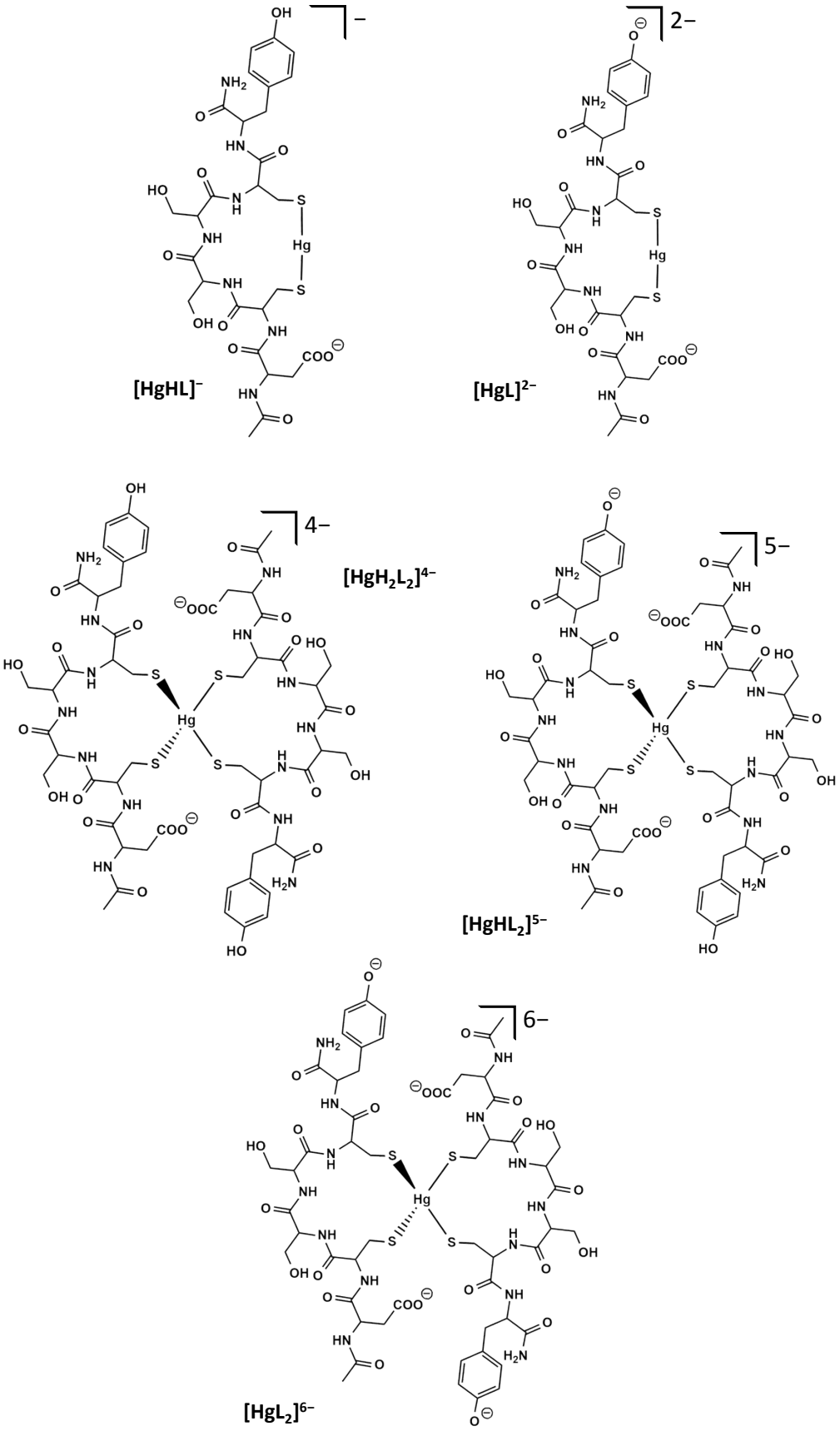

Scheme S1. Proposed schematic structures for the Hg^{2+}:DY complexes.

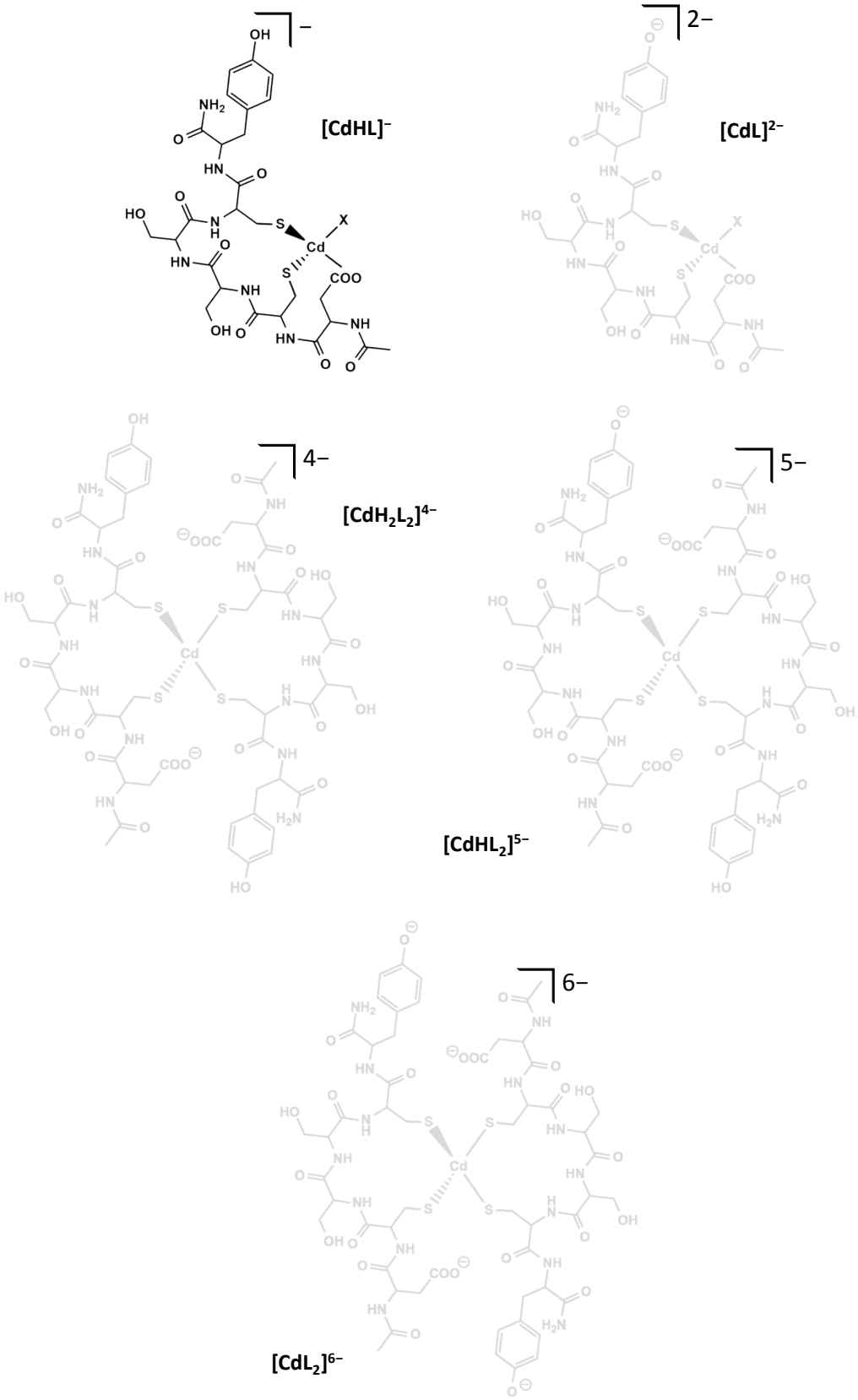

Scheme S2. Proposed schematic structures for the Cd^{2+}:DY complexes. X stands for an oxygen donor from either a H_2O molecule or a possibly coordinating amide carbonyl moiety.